



## Optical and Laser Properties of a Nd doped $\text{LaSc}_3(\text{BO}_3)_4$ Crystal<sup>†</sup>

JUN OH PARK<sup>1</sup>, WON-CHUN OH<sup>2</sup> and WON KWEON JANG<sup>1,\*</sup>

<sup>1</sup>Division of Electronic, Computer and Communication Engineering, Hanseo University, Seosan-si, Chungcheongnam-do, 356-706, South Korea

<sup>2</sup>Department of Advanced Materials Engineering, Hanseo University, Seosan-si, Chungcheongnam-do, 356-706, South Korea

\*Corresponding author: Fax: +82 41 6883352; E-mail: jwk@hanseo.ac.kr

AJC-11354

We discussed about the single  $\text{LaSc}_3(\text{BO}_3)_4$  crystal of the high-temperature phase ( $\alpha$ -phase), which is a strong candidate for highly doped microchip laser material. The crystal structure of  $\text{LaSc}_3(\text{BO}_3)_4$ , a noncentrosymmetric biaxial crystal, was analyzed with its absorption and fluorescent spectra. The energy levels of  $\alpha$ -phased  $\text{LaSc}_3(\text{BO}_3)_4$  were observed in three main transitions with low temperature spectra to remove the phonon induced homogeneous broadening at different pumping wavelengths. The seven weak oscillation lines and oscillation strengths are investigated in Nd ion doped  $\text{LaSc}_3(\text{BO}_3)_4$  crystals of 10 and 15 % doped in doping concentration. The fundamental lasing performance of  $\text{Nd}^{3+}:\text{LaSc}_3(\text{BO}_3)_4$  was observed in a hemispherical resonator structure. The various reflectivity of output couplers was used to get the threshold and intra cavity loss. The beam profile of the laser output was also analyzed for cavity volume estimation. The second harmonic generation was performed by using a nonlinear optical crystal of KTP. The  $\text{Nd}^{3+}:\text{LaSc}_3(\text{BO}_3)_4$  crystal has a broad absorption band of 3 nm at 808 nm, the conventional pumping wavelength with commercial diode laser, provide the easy laser operation and the strong oscillation strength at main laser transition proved in this study also attribute the effective microchip laser fabrication.

**Key Words:** Optical, Laser, Nd,  $\text{LaSc}_3(\text{BO}_3)_4$ .

### INTRODUCTION

Recent trends in laser sources are going to be compact, solid and multi-functional to the remarkable technical progress in the semiconductor industry. An improvement and a modification of a nonlinear device in a semiconductor manufacturing process has been developed for size shrinking and power scale up maintaining the quality of laser output beam simultaneously. New technology such as distributed feedback (DFB), distributed Bragg reflector (DBR), quasi-phase matching (QPM) and periodically poled lithium niobate (PPLN) have been tried for substitution of the conventional diode pumped solid state laser. However, we still have not found a vivid alternative. A microchip laser, in this point, can be a strong candidate for the next reliable laser source that can substitute the conventional solid state laser system. The practical research and development has launched about more than 10 years ago, but the researchers have suffered from problems of a dissipative heat removal and a limitation of power scale up. A microchip laser that can reserve a high laser ion doping concentration in a small volume of gain medium without any crystal defects, is still very attractive in many fields of application even though some technical problems have to be solved.

In this study, we investigated the optical characteristics of Nd:LSB ( $\text{Nd}^{3+}:\text{LaSc}_3(\text{BO}_3)_4$ ) and simulated a theoretical pumping condition for a hemispherical resonator.  $\text{LaSc}_3(\text{BO}_3)_4$ , a biaxial crystal, has some complicated crystal structure. There were about four kinds of the reported crystal energy level diagrams according to the crystal growing conditions. An inarticulate analysis on this complicated energy levels have actually disturbed its practical application<sup>1-3</sup>. We propose, in this study, a more detail energy level analysis on the  $\alpha$ -phase  $\text{LaSc}_3(\text{BO}_3)_4$  crystal with a careful interpretation of the fluorescent spectra with crystal axes. We analyzed stark levels and the oscillation strengths with laser transitions of a crystal and suggested an experimental result for the fundamental and the second harmonic generation in a hemispherical resonator.

### EXPERIMENTAL

**Crystal analysis and optical properties:** There are four kinds of space group in a  $\text{LaSc}_3(\text{BO}_3)_4$  crystal such as  $C2/c$  ( $\alpha$ -phase),  $R32$  ( $\alpha$ -phase),  $Cc$  ( $\alpha$ -phase) and  $C_2$ . The fundamental crystal structure is hexagonal, which usually used for a laser active medium or a nonlinear conversion material. Especially a space group of  $R32$  ( $\alpha$ -phase) showed a self frequency doubling property as reported in YCOB ( $\text{YCa}_4\text{B}_3\text{O}_{10}$ ),

<sup>†</sup>Presented to The 5th Korea-China International Conference on Multi-Functional Materials and Application.

GdCOB ( $\text{GdCa}_4\text{B}_3\text{O}_{10}$ ) and NYAB ( $\text{YAl}_3(\text{BO}_3)_4$ ) crystals. Every space group of  $\text{LaSc}_3(\text{BO}_3)_4$  showed a similar crystal structure but a little different and twisted bonding angle. This little variation of crystal structure changed the energy spacing of Stark levels. The investigated crystal lattice parameters of the C2/c space group are  $a = 7.7 \text{ \AA}$ ,  $b = 9.8 \text{ \AA}$ ,  $c = 12.0 \text{ \AA}$ ,  $\beta = 105.4^\circ$  with a X-ray diffraction instrument (D/MaxIII B, Rigaku Co.)<sup>4-6</sup>.

Table-1 shows the crystal properties of neodymium ion doped crystals that has interested in many laser optic researches.

$\text{Nd}^{3+}:\text{LaSc}_3(\text{BO}_3)_4$  shows a higher doping concentration than other Nd-doped crystals as maintaining optical, mechanical qualities and is easy to polish and grow to a single crystal. It has a wider absorption bandwidth compared to other Nd-doped crystals, which is much favorable to pump with a conventional diode laser for easy wavelength tuning around 808 nm.

Fig. 1 is an experimental setup for measuring fluorescent spectra of a  $\text{Nd}^{3+}:\text{LaSc}_3(\text{BO}_3)_4$  crystal at low temperature environment. The crystal was placed in vacuum chamber and pumped by a optical parametric oscillator (OPO) system. The pumping wavelength was finely tuned to 808 nm of the maximum absorption peak of  $\text{Nd}^{3+}:\text{LaSc}_3(\text{BO}_3)_4$ . The temperature was lowered with two steps of 77 K with liquid nitrogen and 5 K with liquid helium. The pump laser beam focused to the crystal and the fluorescence collected by a data acquisition system.

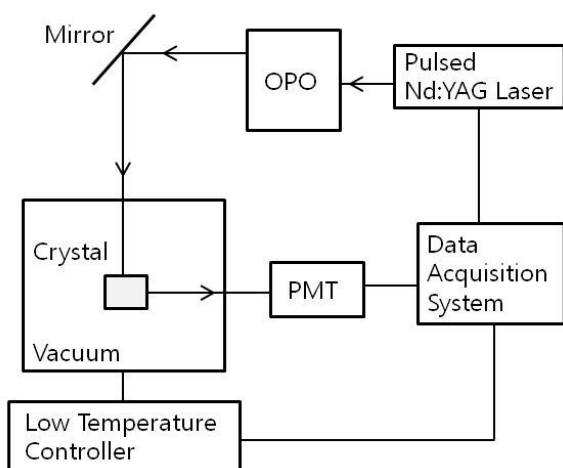


Fig. 1. Experimental setup for measuring fluorescent spectra in low temperature environment

Fig. 2 shows the fluorescent spectra of a  $\text{Nd}^{3+}:\text{LaSc}_3(\text{BO}_3)_4$  crystal at three wavelength regions with various temperature environment. All fluorescent spectra of lower temperature show the sharper peaks than those of higher temperature. At low

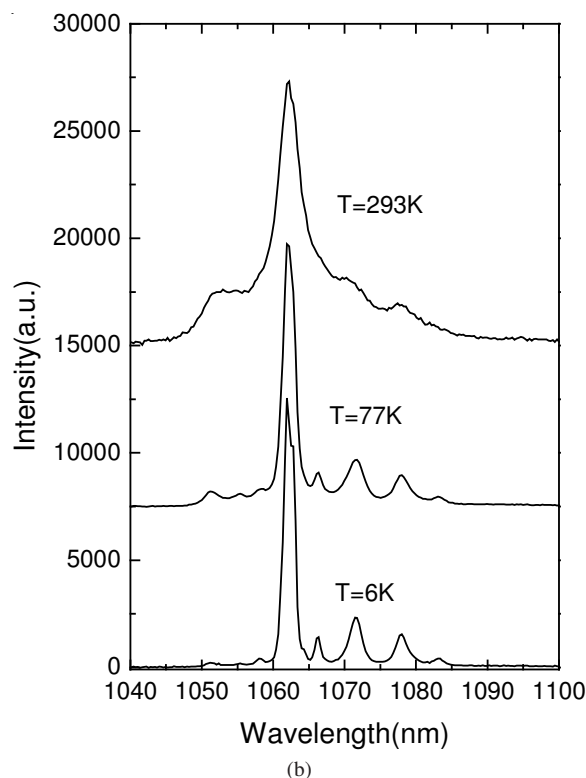
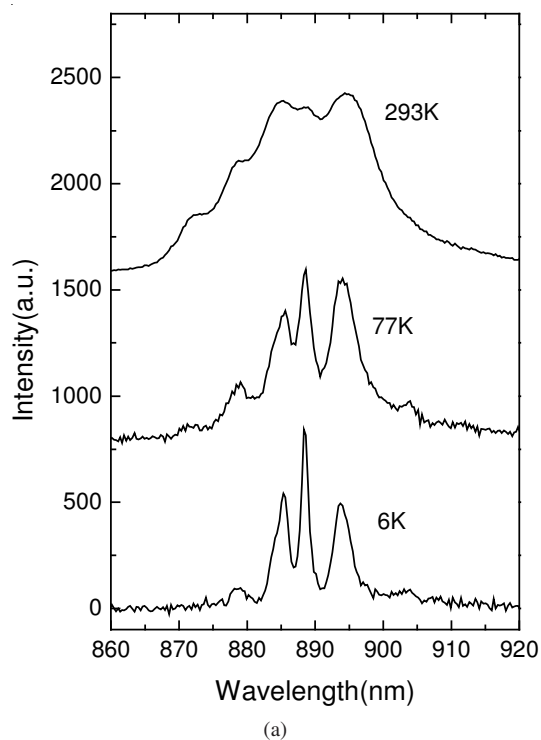


TABLE-1  
COMPARISON OF Nd-TYPE CRYSTALS<sup>7-11</sup>

Property parameter	Nd:LSB	Nd:YVO <sub>4</sub>	Nd:YCOB	Nd:YAG
Doping concentration (%)	15	3.0	5.0	1.1
Melting point (°C)	1600	1825		1950
Mohs hardness	ca. 7	4-5		8.5
Refractive index at 1.06 μm	1.82	1.96(n <sub>o</sub> ), 2.17(n <sub>e</sub> )	1.68(n <sub>x</sub> ), 1.72(n <sub>y</sub> ), 1.73(n <sub>z</sub> )	1.82
Fluorescence lifetime (μs)	118	35.8	95	240
Absorption cross section (cm <sup>2</sup> )	$1.3 \times 10^{-19}$	$9.8 \times 10^{-19}$		$3.3 \times 10^{-19}$
Absorption length (μm)	109.9	90.1		1176.5

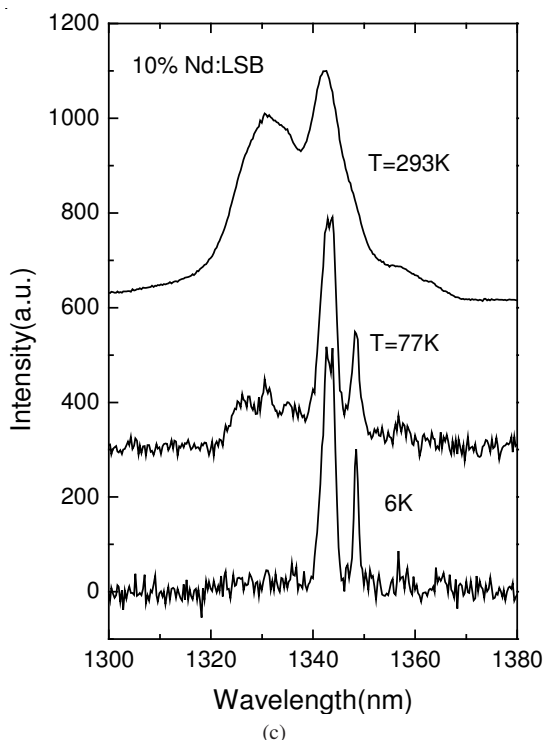


Fig. 2. Fluorescent spectra of a  $\text{Nd}^{3+}:\text{LaSc}_3(\text{BO}_3)_4$  crystal at three different wavelength regions with various temperature environment

temperature environment, the thermal background reduced and Stark levels became vivid. In Fig. 2(a), the fluorescent spectra shows the  ${}^4\text{F}_{3/2} \rightarrow {}^4\text{I}_{9/2}$  transition and three peaks emerged at 878.7, 893.7, 903.4 nm. In case of Nd:YAG six peaks of multi-splitting observed around this region. Compared to that of Nd:YAG crystal the branch ratio of  $\text{Nd}^{3+}:\text{LaSc}_3(\text{BO}_3)_4$  at this transition evaluated to 0.441, which was a little lower than 0.468 of  ${}^4\text{F}_{3/2} \rightarrow {}^4\text{I}_{11/2}$  transition and much higher than 0.086 of  ${}^4\text{F}_{3/2} \rightarrow {}^4\text{I}_{13/2}$  transition. Besides these three transition, the branch ratio of  ${}^4\text{F}_{3/2} \rightarrow {}^4\text{I}_{15/2}$  transition was 0.004, which was difficult to measure due to its low fluorescence and far wavelength of 1.88  $\mu\text{m}$ .

In Fig. 2(b), the strongest oscillation strength was observed at 1061.9 (1062.8) nm with multi-splitting. Three peaks of 1051.2, 1055.2 and 1058.1 nm at shorter wavelength and four peaks of 1066.3, 1071.6, 1077.9 and 1083.1 nm at longer wavelength than 1061.9 nm peak are observed. At shorter wavelength region, one more peak was found than those of a Nd:YAG crystal, but three less peaks were observed in the longer wavelength region whereas Nd:YAG crystal has seven peaks. This reduced number of peaks may be caused by the complicated crystal structure of  $\text{Nd}^{3+}:\text{LaSc}_3(\text{BO}_3)_4$ . It can be assumed that the Stark levels of  $\text{Nd}^{3+}:\text{LaSc}_3(\text{BO}_3)_4$  crystal might be changed and the bonding angle tilted by a crystal growing condition. In  ${}^4\text{F}_{3/2} \rightarrow {}^4\text{I}_{13/2}$  transition of a Nd:YAG crystal, the most prominent Nd-type laser host material, about 9 split peaks were found, but only two peaks of 1342.8 and 1348.8 nm were shown in Fig. 2(c). Multi-splitting, of course, was observed at two strong peaks of 1342.8 and 1348.8 nm.

## RESULTS AND DISCUSSION

**Lasng properties of a  $\text{Nd}^{3+}:\text{LaSc}_3(\text{BO}_3)_4$  crystal:** Fig. 3 shows the hemispherical laser oscillator structure for a highly

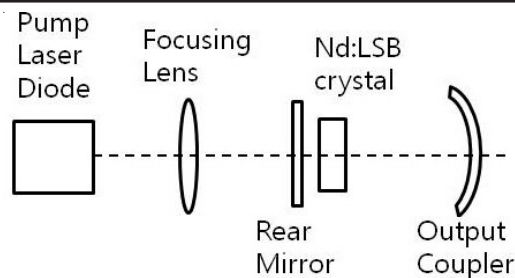


Fig. 3. Laser diode pumped hemispherical laser oscillator

doped  $\text{Nd}^{3+}:\text{LaSc}_3(\text{BO}_3)_4$  microchip laser crystal. In a common structure of a microchip laser oscillator, the rear side of a microchip laser material is usually coated for high transmittance at pump wavelength and high reflectance at laser wavelength simultaneously. However, in our laser oscillator structure, the rear mirror and laser gain medium separated to find the optimum oscillation condition.

We calculated the cavity stability and the cavity beam radius along cavity axis and the results are in Fig. 4. Cavity beam radius was the minimum of 178  $\mu\text{m}$  at the surface of a rear mirror and increased to about 400  $\mu\text{m}$  when the cavity length assumed to be 100 mm. The pumping laser diode beam focused at the point of inside the laser gain material. The cavity stability showed the maximum at the surface of the output coupler and the minimum at the surface of rear mirror.

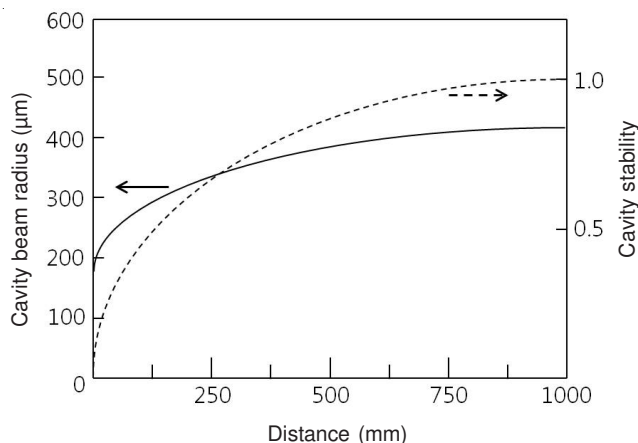


Fig. 4. calculated cavity beam radius and stability along the cavity distance

Fig. 5 shows the fundamental laser output as a function of the absorbed pumping power. The reflectance of a output coupler was 0.97 and the output coupler has the curvature of 100 mm. The pumping wavelength was 808 and 886 nm. The absorption coefficient of 808 nm is much higher than other absorption peaks in the absorption spectra of a  $\text{Nd}^{3+}:\text{LaSc}_3(\text{BO}_3)_4$  crystal. However, in a function of absorbed power, the laser output showed the different results as shown in Fig. 5. The slope efficiency improved from 55-59 % with changing the pumping wavelength from 808-886 nm. The threshold also lowered from 20-6 mW with moving the wavelength from 808-886 nm.

The wavelength of the fundamental laser output was 1063 nm, which was a little shorter than that of Nd:YAG laser. The wavelength moving to longer absorption peak of 886 nm can reduce the quantum defect even though its lower absorption

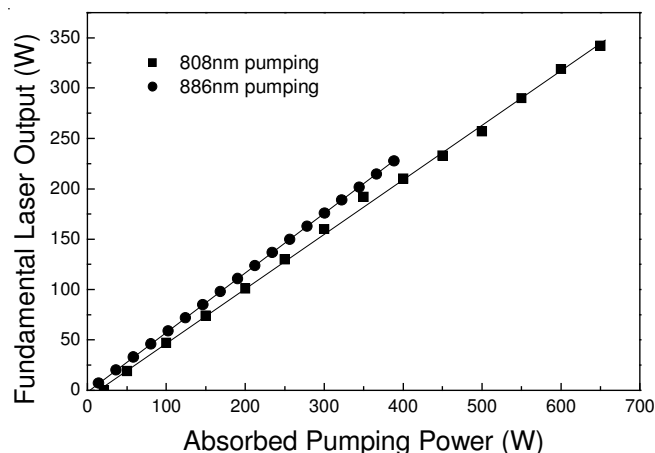


Fig. 5. A fundamental laser output of  $\text{Nd}^{3+}:\text{LaSc}_3(\text{BO}_3)_4$  microchip laser with absorbed power in 808 and 886 nm pumping condition

cross-section of 886 nm than that of 808 nm. In most case, the pumping wavelength for a Nd-type laser material is around 808 nm because it has the biggest absorption cross-section. In function of the pumping power, the pumping with 808 nm produces much higher output power than those of other wavelength pumping. However, the 808 nm pumping also generates larger dissipative heat. In the respect of energy conversion, 886 nm pumping is much higher efficiency<sup>12</sup>.

Fig. 6 is the measured second harmonic generation output with the pump power. A nonlinear optical crystal of KTP used for the frequency conversion. The overall conversion efficiency was low comparing to the second harmonic generation of other Nd-type laser. However, the internal frequency conversion in a microchip scaled has not reported before. The more investigation for an internal frequency conversion should provide an improved conversion efficiency in future.

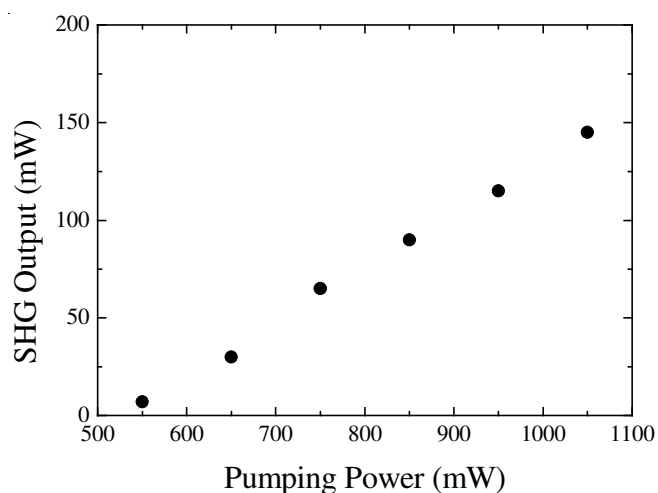


Fig. 6. Second harmonic generation from the  $\text{Nd}^{3+}:\text{LaSc}_3(\text{BO}_3)_4$  laser with pumping power

Fig. 7 is the 3-directional image of the fundamental laser output at 1.063  $\mu\text{m}$ , which seems to be a Gaussian profile. The coarse profile seems to be caused by a short cavity and laser diode pumping. The laser diode intrinsically has a large divergence and worse beam profile than other solid state laser such as Ti: sapphire laser.

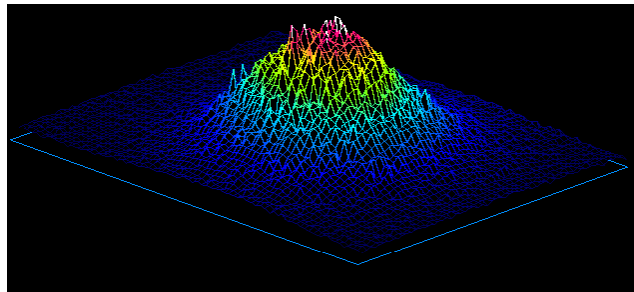


Fig. 7. Beam profile of a  $\text{Nd}^{3+}:\text{LaSc}_3(\text{BO}_3)_4$  microchip laser at 1.06  $\mu\text{m}$

It is believe that a  $\text{Nd}^{3+}:\text{LaSc}_3(\text{BO}_3)_4$  can be fabricated in form of microchip laser due to its excellent gain property even a dense doping concentration and complicated crystal structure.

The optical characteristics of a Nd doped  $\text{LaSc}_3(\text{BO}_3)_4$  crystal as a laser active medium were discussed and investigated its lasing and second harmonic generation properties.

## REFERENCES

1. A. Ikesue, T. Kinoshima, K. Kamata and K. Yoshimura, *J. Am. Ceram. Soc.*, **78**, 1033 (1995).
2. I. Shoji, S. Kurimura, Y. Sato, T. Taira, A. Ikesue and K. Yoshida, *Appl. Phys. Lett.*, **77**, 939 (2000).
3. J. Lu, M. Prabha, J. Song, C. Li, J. Xu, K. Ueda, A.A. Kaminskii, H. Yagi, T. Yanagitani, *Appl. Phys. B*, **71**, 469 (2000).
4. G. Wang, W. Chen, Z. Li and Z. Hu, *Phys. Rev. B*, **60**, 15469 (1999).
5. G. Wang, M. He, W. Chen, Z. Lin, S. Lu and Q. Wu, *Mater. Res. Innovat.*, **2**, 341 (1999).
6. B. Meier, J.-P. Meyn, R. Knappe, K.-J. Boller, G. Huber and R. Wallenstein, *Appl. Phys.*, **58B**, 381 (1994).
7. A.A. Kaminskii, G.A. Bogolubova and L. Li, *Ser. Neorg. Mater.*, **5**, 673 (1969).
8. Z.D. Luo, A.D. Jiang, Y.C. Huang and M.W. Qiu, *Chin. Phys. Lett.*, **3**, 541 (1986).
9. S.A. Kutovoi, V.V. Laptev and S.Y. Matsnev, *J. Quantum. Electron.*, **21**, 131 (1991).
10. T. Taira, A. Mukai, Y. Nozawa and T. Kobayashi, *Opt. Lett.*, **16**, 1955 (1991).
11. I. Shoji, Y. Sato, S. Kurimura, T. Taira, A. Ikesue and K. Yoshida, *Appl. Phys. Lett.*, **77**, 939 (2000).
12. W.K. Jang, T. Taira, Y. Sato and Y.M.n Yu, *Japan. J. Appl. Phys.*, **43**, L70 (2004).